ISSN 1990-7931, Russian Journal of Physical Chemistry B, 2014, Vol. 8, No. 6, pp. 769–782. © Pleiades Publishing, Ltd., 2014.
Published in Russian in Khimicheskaya Fizika, 2014, Vol. 33, No. 11, pp. 12–25.

ELEMENTARY PHYSICOCHEMICAL PROCESSES

A Hard Sphere Model for Direct Three-Body Recombination of Heavy Ions[1]

E. V. Ermolova*, L. Yu. Rusin*, and M. B. Sevryuk**

Talroze Institute of Energy Problems of Chemical Physics, Russia Academy of Sciences, Leninskii pr. 38, building 2, Moscow, 119334 Russia

*e-mail: *rusin@chph.ras.ru; **sevryuk@mccme.ru*

Received June 23, 2014

Abstract—We describe a hard sphere model of direct three-body recombination of the Cs^+ and Br^- ions in the presence of neutral atoms Hg, Xe, Kr, or Ar as the third bodies. Calculations are carried out for the ion approach energy and the third body energy in the range from 1 to 10 eV under the assumption of non-central approach of the ions. The calculation results include the dependences of the total recombination probability on these energies as well as the opacity functions for two impact parameters and the dependences of the recombination probability on the angles determining the mutual orientation of the velocities of the reagents. The classification of the three-body collisions according to the sequences of pairwise encounters of the particles is considered. The most widespread mechanism of energy removal from the ionic pair is a single impact of the third body with the Br^- ion.

Keywords: direct three-body recombination, hard sphere model, ionic pair, opacity functions, types of three-body collisions

DOI: 10.1134/S1990793114110037

1. INTRODUCTION

Three-body recombination reactions $A + B + R \rightarrow AB + R$ (here R is the acceptor of excess kinetic energy of the A + B pair) as well as reverse reactions of collision induced dissociation (CID) play a major role in many complicated chemical processes in plasma and in other media of natural or artificial origin. For instance, the survey [1] considers 196 elementary gas phase reactions used in modeling combustion processes, and about a half of them are recombination or CID reactions [2, 3]. Quantum mechanical simulation of the recombination process $Ne + Ne + H \rightarrow Ne_2 + H$ under various temperatures and pressures carried out in the works [2–6] has shown that for this reaction, *direct* recombination where all the three reagent atoms collide simultaneously or almost simultaneously prevails over the mechanisms based upon successive two-body encounters. As one expects, predominance of the direct mechanism of the reaction is especially noticeable under high pressures [4, 5]. After the papers [2–6], an interest in the processes of direct three-body recombination and, in particular, in the problems of examining their dynamics increased considerably. Experimental investigation of the dynamics of direct three-body recombination reactions in crossed molecular beams is beyond the possibilities of the contemporary experimental techniques. Therefore, the only way of studying the dynamics of such reactions is simulation by various quantum mechanical or quasiclassical methods.

One of the most important classes of three-body recombination reactions is recombination of ions. The competition of the processes of recombination of ions and ionic dissociation of molecules is one of the factors determining the concentration of ions in plasma. In the works [7–20], we performed a detailed investigation of the dynamics of direct three-body recombination of heavy ions

$$Cs^+ + Br^- + R \rightarrow CsBr + R \quad (1)$$

(R = Hg, Xe, Kr) via quasiclassical trajectory simulation (quantum effects in the processes (1) are negligibly small). The choice of the systems (1) was caused mainly by the fact that the diabatic potential energy surfaces (PESs) of the reverse CID reactions

$$CsBr + R \rightarrow Cs^+ + Br^- + R,\ CsR^+ + Br^- \quad (2)$$

(R = Hg, Xe, Kr) have been reliably determined and allow one to reproduce quantitatively in trajectory calculations all the experimental data obtained in crossed molecular beams (the works [7–20] contain the relevant references). According to the microscopic reversibility principle, the processes (1) and (2) reverse with respect to each other are governed by the same PES (different for different atoms R). In particular, in the works [7–20], for various values of the ion approach energy E_i and the third body energy E_R (mainly in the

[1] The article was translated by the authors.

range from 1 to 10 eV), we calculated the recombination probabilities for the collisions $Cs^+ + Br^- + R$, discovered several dynamical mechanisms of recombination along with a description of the mass and orientation effects, and found the minimum possible internal energy E_{min} of the nascent CsBr molecule. Finally, in the space of the initial conditions (kinematic parameters) of the collisions, we determined the region yielding recombination. It was assumed in most of the works that the ion approach is central (i.e. that the impact parameter b_i of the ions is equal to zero), but collisions with non-central ion approach ($b_i > 0$) were considered as well [13, 18, 19]. In the paper [18], two-stage direct three-body recombination (1) with R = Xe was explored where the stage of energy removal from the recombining pair is delayed with respect to the instant when the interionic distance attains its minimal value.

The recombination processes (1) for different atoms R differ in the third body mass as well as in the topography of the PES involved. To separate the mass effects from the effects related to the structure of the potential energy surface, in the thesis [19] and the paper [20], we considered six imaginary "cross" reactions for which the PES governing the motion of the particles and the third body mass correspond to different atoms R = Hg, Xe, Kr. As was revealed in those works, the effectivities of the mercury and xenon atoms as stabilizers of the nascent CsBr molecule are quite close, depend slightly on the PES used, and exceed significantly the effectivity of the krypton atom, despite an almost exact equality of the mass ratios $m_{Hg}/m_{Xe} = 1.528$ and $m_{Xe}/m_{Kr} = 1.567$.

The easiest way to exclude completely the effect of the PES relief on various reaction characteristics is to consider the *hard sphere model* of the process, where a vertical wall (in combination with Coulomb attraction or repulsion if there are ions among the interacting particles) is used as the potential. Otherwise speaking, in the framework of the hard sphere model, the particles involved in the process are treated as balls exchanging energies and momenta at their encounters with each other according to the elastic impact law. In the theory of atomic and molecular collisions, various versions of the hard sphere model are used rather widely, see e.g. the works [21–28] and references therein. In the recent paper [29], the hard sphere model is applied for studying the three-body recombination $He + He + He \rightarrow He_2 + He$.

In the present work, we propose a hard sphere model of direct three-body recombination of ions

$$Cs^+ + Br^- + R \rightarrow CsBr + R \qquad (3)$$

(R = Hg, Xe, Kr, Ar) and describe the calculation results. Full trajectory simulation of recombination of the Cs^+ and Br^- ions with an argon atom as the third body was not carried out because of the absence of an adequate PES tested carefully, but within the framework of the hard sphere model, an Ar atom can be considered along with Hg, Xe, and Kr atoms. It is worthwhile to emphasize that our model excludes a simultaneous encounter of all the three particles and even a simultaneous encounter of the neutral atom with both the ions (an occurrence of these events requires a special choice of initial conditions). On the contrary, it is supposed that only pairwise encounters of the balls representing the particles Cs^+, Br^-, and R happen in the system.

Quasiclassical trajectory calculations enable one to obtain an almost accurate dynamical portrait of the elementary process (provided that the PES employed is sufficiently adequate and quantum effects are sufficiently small which does hold in the case of the reactions (1)). Hard sphere model describes the interaction of the particles only approximately, but it is of considerable theoretical interest since it allows one to examine the role of the particle masses and other kinematic parameters of the collision irrespective of the PES structure [23, 27]. Moreover, as we will see, many results of the trajectory and hard sphere calculations for the reactions (1) turn out to be qualitatively the same.

2. DESCRIPTION OF THE MODEL

Each of the particles Cs^+, Br^-, Hg, Xe, Kr, and Ar was represented by a ball of the mass corresponding to the actual atomic weight of the element in question. As the radii of the balls, we used the ionic radii of Cs^+ and Br^- ions (1.67 and 1.96 Å, respectively [30]) and the atomic radii of neutral atoms Hg, Xe, Kr, and Ar (1.55 [31], 2.18 [32], 1.98 [32], and 1.92 Å [33], respectively). It was assumed that at a contact of any two balls, their velocities change according to the elastic impact law [21–28], while in the time intervals between the encounters, the neutral atom R moves inertially (under no forces) and the Cs^+ and Br^- ions move under Coulomb attraction. As was already pointed out in the introduction, the probability of a simultaneous encounter of one of the particles with the two others vanishes.

The general setup of non-central approach of the ions was considered, with the impact parameter b_i of the ions ranging from zero to a certain maximal value $b_{i\,max}$ and with the impact parameter b_R of the atom R (with respect to the center of mass of the ionic pair) ranging from zero to a certain maximal value $b_{R\,max}$. For each of the four atoms R, at fixed values of the ion approach energy E_i (the initial kinetic energy of the relative motion of the ions), the third body energy E_R (the initial kinetic energy of the relative motion of the atom R and the ionic pair), and the maximal impact parameters $b_{i\,max}$ and $b_{R\,max}$, the initial conditions of the collision were selected, on the whole, in the same way as in the paper [13] devoted to trajectory simulation of the process of one-stage direct three-body recombination (1) with R = Xe for non-central approach of the ions.

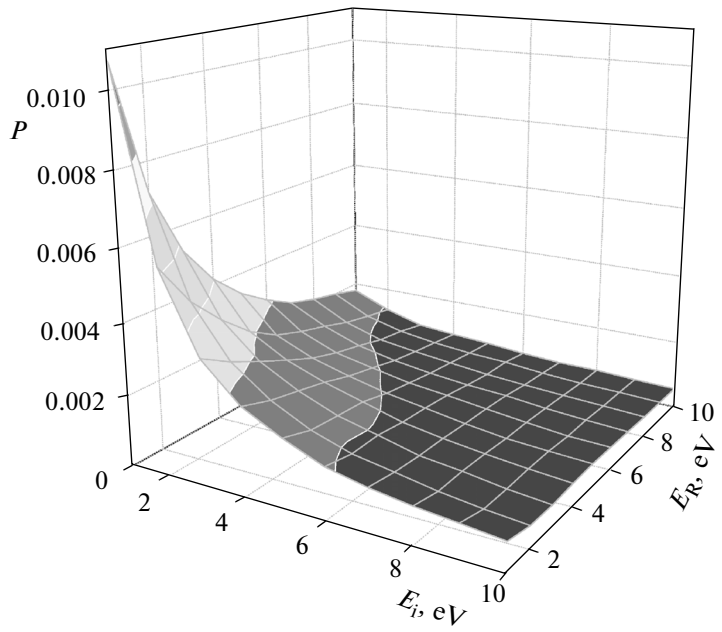

Fig. 1. The dependence of the total recombination probability P on the energies E_i and E_R in case **2** for R = Hg.

Since the selection procedure for the initial conditions is very important, we will describe it in detail (cf. Fig. 1 in [13]). We assumed that at the initial time instant $t = 0$, the center of mass of the ionic pair coincides with the origin of the fixed coordinate frame $Oxyz$ and has zero velocity whereas the distance between the nuclei of the ions is equal to $d_i = 250$ Bohr $> b_{i\,max}$, as we had done in the trajectory simulation of the processes (1) [7–20]. The initial vector $\mathbf{v}_i$ of the relative velocity of the ions (to be more precise, of the velocity of the Cs^+ ion with respect to the Br^- ion) was selected according to the formula

$$\mathbf{v}_i = (2E_i/\mu_i)^{1/2}(e_x, e_y, e_z),$$

where μ_i is the reduced mass of the ions,

$$e_x = \cos\Theta,\ e_y = \sin\Theta\cos\Phi,\ e_z = \sin\Theta\sin\Phi,$$

Θ is the polar angle of the vector $\mathbf{v}_i$ with respect to the Ox axis ($0 \le \Theta \le \pi$), and Φ is the corresponding azimuthal angle ($0 \le \Phi < 2\pi$). The initial vector $\mathbf{r}_i$ connecting the ion nuclei and directed from Br^- to Cs^+ was selected according to the formula

$$\mathbf{r}_i = -(d_i^2 - b_i^2)^{1/2}(e_x, e_y, e_z) + (b_i\cos\gamma)(f_x, f_y, f_z) + (b_i\sin\gamma)(g_x, g_y, g_z),$$

where

$$f_x = -\sin\Theta,\quad f_y = \cos\Theta\cos\Phi,\quad f_z = \cos\Theta\sin\Phi,$$

$$g_x = 0,\quad g_y = \sin\Phi,\quad g_z = -\cos\Phi,$$

and γ is the orientation angle characterizing the position of the plane spanned by the vectors $\mathbf{v}_i$ and $\mathbf{r}_i$ ($0 \le \gamma < 2\pi$). It is easy to see that the vectors (e_x, e_y, e_z), (f_x, f_y, f_z), and (g_x, g_y, g_z) are of unit length and pairwise orthogonal.

Now consider two material points with the reduced mass equal to μ_i that move along a straight line under Coulomb attraction with the potential $-1/r$ (in the atomic units) where r is the distance between the points. Suppose that at the initial time instant, the equality $r = d_i$ holds and the points are moving towards each other with relative kinetic energy E_i and with the total energy $E_{tot} = E_i - 1/d_i > 0$. It is not hard to verify that such points will meet each other in the time equal to

$$\tau = \tau(d_i, E_i, \mu_i) = (\mu_i/2)^{1/2} E_{tot}^{-3/2}[AB - \ln(A + B)] \quad (4)$$

(in the atomic units) where the notation $A = (d_i E_{tot})^{1/2}$ and $B = (d_i E_{tot} + 1)^{1/2}$ is used. In the paper [7], we presented a more complicated version of the formula (4) with a wrong sign: the equation (13) in [7] actually gives the value $-\tau(d_i, E_i, \mu_i)$. We assumed that the initial vector $\mathbf{v}_R$ of the velocity of the atom R is equal to

$$\mathbf{v}_R = (-v_R, 0, 0),\quad v_R = (2E_R/\mu_R)^{1/2},$$

where μ_R is the reduced mass of the ionic pair and the atom R, while the initial position of the nucleus of this atom is given by the radius vector

$$\mathbf{r}_R = (v_R\tau, b_R, 0).$$

Thus, in the hypothetical situation where the radii of the particles and the impact parameter b_i are equal to

zero, the atom R flying along a straight line parallel to the Ox axis would reach the Oyz plane at the same instant $t = \tau$ as the ions would collide at the origin (the condition defining a one-stage process in the sense of the paper [18]).

Besides the energies E_i and E_R (and the particle masses), the kinematic parameters in this procedure are the impact parameters b_i, b_R and the angles Θ, Φ, γ. These parameters were selected according to the standard formulas

$$b_i = b_{i\,max}\xi_1^{1/2}, \quad b_R = b_{R\,max}\xi_2^{1/2},$$
$$\cos\Theta = 2\xi_3 - 1, \quad \Phi = 2\pi\xi_4, \quad \gamma = 2\pi\xi_5, \tag{5}$$

where ξ_1, ξ_2, ξ_3, ξ_4, ξ_5 are independent random variables uniformly distributed between 0 and 1. If for a current collection of the values of the parameters b_i, b_R, Θ, Φ, γ, the initial distance between the nuclei of some two reagents turned out to be smaller than the sum of their radii, then such a collection was rejected and the parameters b_i, b_R, Θ, Φ, γ were selected again.

Note that, as in other problems, direct three-body recombination can be studied using other collections of kinematic parameters. In the works [13, 18, 19], while selecting the initial conditions of trajectories for non-central approach of the ions, the kinematic parameters b_i and γ were given by means of two auxiliary angles Θ_A and Φ_A.

In the time intervals between the encounters of the balls representing the particles Cs^+, Br^-, and R, the atom R and the center of mass of the ionic pair move under no forces (as was pointed out above), whereas the relative motion of the ions was determined by solving numerically the Newtonian equations corresponding to a material point of mass μ_i on a plane (orthogonal to the constant angular momentum vector $\mathbf{M} = \mu_i[\mathbf{r}, \dot{\mathbf{r}}]$) in the field with potential $-1/r$. Here $\mathbf{r}$ is the vector connecting the nuclei of the ions while r is the length of the radius vector of the material point.

Of course, the motion of a mass point in a Coulomb potential (the Kepler problem) can be described analytically [34–36]. We preferred numerical integration of the equations of motion by the following two reasons. First, the analytic solution of the Kepler problem is not an expression of the point coordinates in terms of the time t. Instead, it is an expression of the time in terms of a special parameter u (the eccentric anomaly) that determines the point location on the orbit [34–36] (note a misprint in the well known monograph [35]: on page 70 in the formulas expressing t in terms of u, instead of $n = \pm\gamma^{1/2}p^{-3/2}$, one should read $n = \pm\gamma^{1/2}a^{-3/2}$). To find u as a function of the time t, one has to solve additionally the suitable transcendental Kepler equation [35, 36]. Second, numerical solutions of the equations of motion enable one to avoid considering numerous cases concerning the motion of the point along conic sections of different types—an ellipse, hyperbola, parabola, and straight line (the probability of moving along a parabola or straight line is infinitesimal, though). Notice that in an overwhelming majority of the works devoted to various methods of finding the eccentric anomaly as a function of the time, only elliptic orbits are considered (see e.g. the recent paper [37] and references therein).

The Newtonian equations of motion were integrated by the sixth order Adams–Bashforth method, while the first five integration steps (after selecting the initial conditions or after the latest encounter of two particles) were carried out by the fourth order Runge–Kutta method. The integration step length was set to be equal to 10 au. This has turned out to be enough for very accurate conservation of the total energy and angular momentum of the ionic pair between two consecutive encounters (about 15 significant digits). The precise instant of the impact was determined by a series of trial one-step backward integrations of the equations of motion by the fourth order Runge–Kutta method.

If the total internal energy $E_{tot} = \frac{1}{2}\mu_i\dot{\mathbf{r}}^2 - 1/r$ of the ionic pair between two successive encounters of the particles is negative, then the corresponding material point of mass μ_i moves along an ellipse, if this energy is positive, then the point moves along a hyperbola. Within all the complex of the calculations described below, the minimal eccentricity of such an ellipse was equal to 0.0008724, while the maximal one differed from unity by a quantity smaller than 5×10^{-7}. The minimal eccentricity of a hyperbola differed from unity by a quantity smaller than 5×10^{-6} while the maximal one was equal to 113.7.

Denote by r_0^+ and r_0^- the initial distances between the nucleus of the atom R and the nuclei of the Cs^+ and Br^- ions, respectively. The integration of the equations of motion was stopped and the program proceeded to selecting the next collection of the values of the kinematic parameters b_i, b_R, Θ, Φ, γ as soon as the minimum of the two distances between the nucleus of the atom R and the nuclei of the ions became larger than $\max(r_0^+, r_0^-) + 100$ Bohr. If at this instant the total internal energy E_{tot} of the ionic pair turned out to be negative, recombination of the Cs^+ and Br^- ions was regarded as having occurred (irrespective of the current distance between the ion nuclei). While using the hard sphere model, one has to distinguish clearly between a three-body *collision* of the particles (such a collision is understood as the whole process of interaction of the Cs^+ and Br^- ions and the atom R from the initial time instant $t = 0$ to the termination of integrating the equations of motion) and pairwise elastic *encounters* of the particles (there can be many such encounters within a single collision event).

For each of the four atoms R = Hg, Xe, Kr, Ar, we varied each of the energies E_i and E_R in the interval from 1 to 10 eV with a step of 1 eV. It was these ranges

Table 1. Some characteristics of the recombination process within the framework of the hard sphere model

The third body R	Hg	Xe	Kr	Ar	Hg	Xe	Kr	Ar
	case **1**				case **2**			
$P(E_i = E_R = 1\ \text{eV})$	0.08135	0.09865	0.07814	0.05432	0.01074	0.01373	0.01123	0.00775
$\frac{P(E_i = E_R = 1\ \text{eV})}{P(E_i = 1\ \text{eV}, E_R = 10\ \text{eV})}$	5.40	4.74	3.66	2.02	6.04	5.34	3.96	2.11
$\frac{P(E_i = E_R = 1\ \text{eV})}{P(E_i = 10\ \text{eV}, E_R = 1\ \text{eV})}$	13.2	14.3	19.3	183.5	13.7	16.5	28.1	387.7
$\frac{P(E_i = E_R = 1\ \text{eV})}{P(E_i = E_R = 10\ \text{eV})}$	18.6	18.3	18.0	19.5	19.1	19.0	21.1	23.9
p_i^* for $E_i = E_R = 1\text{eV}$	0.04642	0.05896	0.04755	0.03402	0.00305	0.00457	0.00373	0.00209
$\langle p_i^* \rangle$	0.00488	0.00653	0.00577	0.00500	0.00041	0.00055	0.00046	0.00036
p_R^* for $E_i = E_R = 1$ eV	0.01505	0.02043	0.01433	0.00936	0.00256	0.00325	0.00264	0.00221
$\langle p_R^* \rangle$	0.00296	0.00400	0.00332	0.00269	0.00029	0.00037	0.00032	0.00033
q_i^* for $E_i = E_R = 1$ eV	5.551	5.815	5.920	6.093	1.415	1.660	1.656	1.341
$\langle q_i^* \rangle$	2.997	3.008	2.777	2.263	1.200	1.109	0.864	0.538
q_R^* for $E_i = E_R = 1$ eV	3.503	3.921	3.471	3.262	2.327	2.315	2.297	2.786
$\langle q_R^* \rangle$	4.699	5.227	5.734	6.963	1.941	1.943	2.034	3.434
$\langle \beta \rangle$ for $P^{part}(b_i)$	0.10	0.46	0.67	2.41	3.57	4.34	6.30	9.80
$\langle \beta \rangle$ for $P^{part}(b_R)$	0.00	0.00	0.01	0.34	0.81	1.08	1.19	2.23
$\langle \beta \rangle$ for $P^{part}(\Theta)$	4.27	7.50	14.37	19.30	9.14	17.83	21.76	21.67
$\langle \tilde{\beta} \rangle$ for $P^{part}(\Phi)$	9.13	9.35	8.96	8.92	17.81	16.09	16.37	21.46
Z_{-13}, in per cent	35.75	34.60	33.66	30.69	41.90	40.45	39.93	36.37
Z_{-23}, in per cent	44.57	45.36	50.70	59.40	47.34	48.85	52.55	59.36

Angle brackets denote the mean value over all the 100 pairs of energies (E_i, E_R).

of the energies E_i and E_R that were used in most of the works [7–20] on trajectory simulation of direct three-body recombination (1), although we also considered larger [7, 9, 10] and smaller [7–10, 13, 18] values of the energies. Recall that in gas-discharge plasma (the most representative example of low temperature plasma [38]), a typical temperature of the electronic component ranges between 0.5 and 7 eV (in the units of k^{-1}), whereas the gas temperature (and, consequently, the temperature of the ionic component) ranges between 0.03 and 3 eV (see Table 1.2 in the manual [39]).

For each atom R and for each pair of energies (E_i, E_R), we generated $N = 500000$ events of three-body collision (3) with $b_{i\,max} = 40$ Bohr, $b_{R max} = 20$ Bohr (these maximal values of the impact parameters were used in the paper [13]) and 500000 three-body collision events with doubled values $b_{i\,max} = 80$ Bohr, $b_{R\,max} = 40$ Bohr. In the sequel, calculations with $b_{i\,max} = 40$ Bohr and $b_{R\,max} = 20$ Bohr will be referred to as case **1**, while calculations with $b_{i\,max} = 80$ Bohr and $b_{R\,max} = 40$ Bohr will be referred to as case **2**.

In each of cases **1** and **2**, for each of the four atoms R and for each pair of energy values (E_i, E_R), we computed the total recombination probability $P = N_0/N$ as the ratio of the number N_0 of three-body collision events ending in recombination of the ions (such collisions will be said to be *recombinative*) to the number $N = 500000$ of all the three-body collision events generated. The adequacy of such a method for finding the

Table 2. The types of recombinative three-body collisions

Number of collisions	In per cent	Type
1521776	49.56	(−23)
1060178	34.53	(−13)
150762	4.910	(13, −23)
145311	4.733	(23, −13)
89433	2.913	(12, −23)
46057	1.500	(−23, −13)
26039	0.848	(12, −13)
19845	0.646	(−13, −23)
5010	0.163	(13, 12, −23)
2765	0.0901	(23, 12, −23)
875	0.0285	(23, −13, −23)
861	0.0280	(23, 12, −13)
374	0.0122	(13, 12, −13)
330	0.0107	(−23, −13, −23)
327	0.0106	(13, −23, −13)
269	0.0088	(23, 13, −23)
104	0.0034	(−23, −12, −13)
59	0.0019	(−13, −12, −23)
30	0.00098	(23, −23)
17	0.00055	(−23, 13, −23)
16	0.00052	(−13, −23, −13)
16	0.00052	(13, 23, −13)
11	0.00036	(13, 23, 12, −23)
8	0.00026	(−23, −12, −23)
4	0.00013	(23, 23, −13, −23)
2	6.5×10^{-5}	(−13, 23, −13)
2	6.5×10^{-5}	(13, −23, −12, −23)
2	6.5×10^{-5}	(23, 23, 23, −13, −23)
1	3.3×10^{-5}	(23, 23, −13)
1	3.3×10^{-5}	(23, 23, 12, −23)
1	3.3×10^{-5}	(23, 23, 13, −23)
1	3.3×10^{-5}	(−23, −13, −12, −13)
1	3.3×10^{-5}	(23, 13, 12, −13)
1	3.3×10^{-5}	(23, −13, −23, −13)

The number of collisions in per cent is given with respect to the total number of recombinative collisions, 3070489.

recombination probability follows from the formulas (5) which correspond to uniform distributions of the quantities b_i^2, b_R^2, $\cos\Theta$, Φ, and γ. Moreover, we determined the dependences of the recombination probability on each of the kinematic parameters b_i, b_R, Θ, and Φ. To this end, the range of the parameter at hand ($0 \le b_i \le b_{i\,max}$, $0 \le b_R \le b_{R\,max}$, $0° \le \Theta \le 180°$, and $0 \le \Phi < 360°$) was divided into a sufficiently large number of equal subintervals (of a length of 2 Bohr, 2 Bohr, 5°, and 10° for b_i, b_R, Θ, and Φ, respectively), and then the ratios $P^{part} = N_0^{part} / N^{part}$ were computed, where N^{part} (N_0^{part}) is the number of all the three-body collisions generated (that of the recombinative collisions, respectively), for which the value of the parameter in question lies inside the subinterval under consideration. For the impact parameter b_i, we will also write $P^{part}(b_i) = N_0^{part}(b_i) / N^{part}(b_i)$ regarding b_i in this equality as the middle of the subinterval under consideration, and similar notation will also be used for the kinematic parameters b_R, Θ, and Φ. For instance, the middle of the last subinterval for b_i is $b_{i\,max} - 1$ Bohr, and that for b_R is $b_{R\,max} - 1$ Bohr. According to the formulas (5), $N^{part}(\Phi)$ is almost independent of Φ, whereas the quantities $N^{part}(b_i)$, $N^{part}(b_R)$, and $N^{part}(\Theta)$ are approximately proportional to b_i, b_R, and $\sin\Theta$, respectively. Since our selection procedure for the initial conditions of a three-body collision is symmetric with respect to the *Oxy* plane, the approximate equality $P^{part}(\Phi) \approx P^{part}(360° - \Phi)$ holds for any angle Φ. We did not examine the dependence of the recombination probability on the orientation angle γ.

Recall that the dependences $P^{part}(b_i)$ and $P^{part}(b_R)$ of the recombination probability on the impact parameters are called the *opacity functions*, see the thesis [10] and references therein. It is important to note that the opacity function in b_i depends on $b_{R\,max}$ and the opacity function in b_R depends on $b_{i\,max}$.

3. RESULTS OF THE CALCULATIONS

One of the most important characteristics of direct three-body recombination is the dependence of the total recombination probability P on the ion approach energy E_i and the third body energy E_R. In Table 1, for R = Hg, Xe, Kr, Ar and for both cases **1** and **2**, we present the probability P for the lowest values of these energies, $E_i = E_R = 1$ eV, as well as the ratios of the recombination probability at $E_i = E_R = 1$ eV to the recombination probabilities at $E_i = 1$ eV, $E_R = 10$ eV, at $E_i = 10$ eV, $E_R = 1$ eV, and at $E_i = E_R = 10$ eV. As is seen in Table 1, at $E_i = E_R = 1$ eV in both cases **1** and **2**, the heavier the third body R is (and, consequently, the stronger on the average the total internal energy E_{tot} of the ionic pair changes at an encounter of the atom R

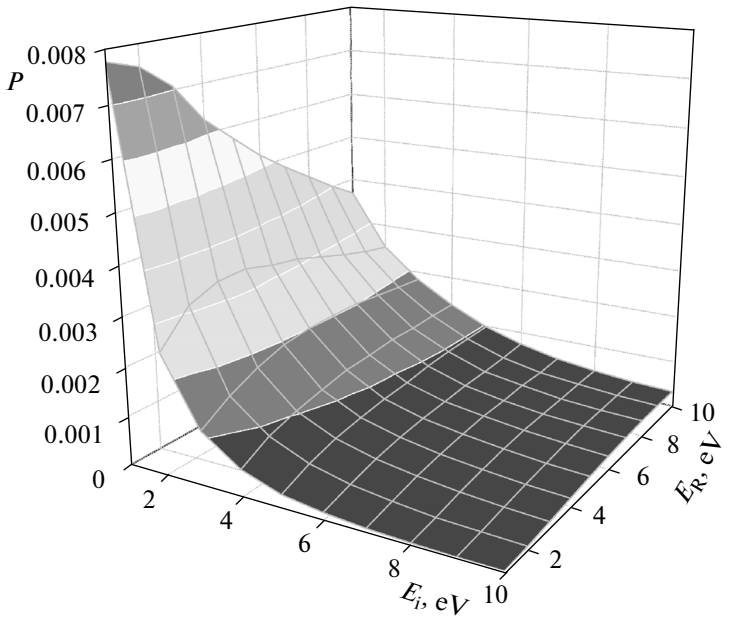

Fig. 2. The dependence of the total recombination probability P on the energies E_i and E_R in case **2** for R = Ar.

with one of the ions), the higher is the probability P, on the whole. An increase in the recombination probability as one passes from Hg to Xe is caused by the fact that the atomic radius of a mercury atom is significantly smaller than that of an atom of any of the three inert gases considered [31–33]. The heavier the third body is, the faster the probability P decreases as E_R grows at the fixed energy $E_i = 1$ eV. On the other hand, one observes the opposite trend as E_i increases at $E_R =$ 1 eV, namely, the heavier the third body is, the more slowly the recombination probability decreases (but this decrease is always much stronger than that as E_R grows for $E_i = 1$ eV). On the whole, for each of the four atoms R, the functions $P(E_i, E_R)$ in case **1** and in case **2** are very similar (up to a certain proportionality factor, see below). Figures 1 and 2 show the dependences of the recombination probability P on the energies E_i and E_R in case **2** for R = Hg and R = Ar, respectively.

As our calculations prove, the recombination probability P depends on E_i much stronger than on E_R. Therefore, at any fixed value of the third body energy E_R, the probability P decreases monotonously as the ion approach energy E_i grows, for each of the four atoms R in both cases **1** and **2**. On the other hand, we observed pairs (E_i, E_R) of values of the energies $E_i \geq 2$ eV and $E_R \leq 9$ eV for which $P(E_i, E_R + 1\text{ eV}) > P(E_i, E_R)$. The existence of such pairs cannot be attributed to statistical errors: the almost inexplicable trend of an increase in the recombination probability as the third body energy E_R grows manifests itself regularly. The higher E_i, the lower E_R, and the lighter the atom R is, the stronger this trend is pronounced, on the whole. For instance, for R = Ar in both cases **1** and **2**, for $5 \leq E_i \leq 10$ eV, the probability P increases monotonously as E_R rises in the interval $1 \leq E_R \leq 8$ eV, while for $E_i =$ 10 eV, it increases monotonously in the whole interval $1 \leq E_R \leq 10$ eV (see Fig. 2).

A comparison of the function $P(E_i, E_R)$ for R = Xe in case **1** with the results of the trajectory calculations carried out for R = Xe at the same values $b_{i\,max} = 40$ Bohr, $b_{R\,max} = 20$ Bohr of the maximal impact parameters (see Fig. 2b in the paper [13]) shows an approximate equality of the "trajectory" and "hard sphere" recombination probabilities. For instance, at $E_i = E_R = 1$ eV, the "hard sphere" probability P is equal to 0.09865 (see Table 1) and the "trajectory" one is slightly less than 0.09. The axes labels $E_{ini}(Cs^+–Br^-)$ (E_i in the notation of the present paper) and E_{rel}(Xe–CsBr) (E_R in the notation of the present paper) in the histogram of Fig. 2b in [13] are interchanged. Taking this misprint into account, Fig. 2b in [13] allows us to conclude that for R = Xe, like the "hard sphere" recombination probability, the "trajectory" recombination probability P decreases much faster as E_i grows at fixed small values of E_R than as E_R increases at fixed small values of E_i.

Note that Fig. 2a in the paper [18] shows a histogram of the function $P(E_i, E_R)$ for R = Xe obtained in trajectory calculations with $b_{i\,max} = 40$ Bohr and $b_{R\,max} =$ 100 Bohr. Since recombination with R = Xe is virtually absent in trajectory simulation of the one-stage processes (1) for $b_R > 20$ Bohr, the ratio P(Fig. 2b in [13])/P(Fig. 2a in [18]) is equal to $(100/20)^2 = 25$ for all values of E_i and E_R with a high accuracy.

Another extremely important characteristic of direct three-body recombination is the dependence of the minimum possible total internal energy E_{min} of the molecule obtained on the ion approach energy E_i and the third body energy E_R. The function $E_{min}(E_i, E_R)$ is

more sensitive to the process dynamics than $P(E_i, E_R)$ because it involves no averaging over kinematic parameters. For each atom R and for all the pairs of energies (E_i, E_R), we determined the minimum E_0 of the total internal energy of the resulting bound pair of the Cs^+ and Br^- ions over all the recombinative three-body collisions we generated. However, for all atoms R, the minimum E_0 we found turned out to depend on the energies E_i and E_R in a rather chaotic manner in case **1** as well as in case **2**. This fact enables one to conclude that E_0 exceeded considerably the real minimum E_{min} almost always. To find E_{min}, one has either to generate a much larger number, by orders of magnitude, of three-body collision events for each energy pair (E_i, E_R) or to make use of gradient-free optimization methods well known in numerical analysis [19, 40–42] for functions in many variables. The objective function here is the dependence of the total internal energy of the resulting bound pair of the Cs^+ and Br^- ions on the kinematic parameters of the collisions. Within the framework of trajectory simulation of direct three-body recombination (1), the second approach was successfully employed for central [12, 13, 16, 17, 19, 20] as well as for non-central [13, 19] approach of the ions. Note, however, that in the calculations described in the present work, the inequality $E_0(\text{case } \mathbf{1}) < E_0(\text{case } \mathbf{2})$ held for almost all R, E_i, and E_R. This fact allows one to conjecture that the real minimum E_{min} is attained at $b_i < 40$ Bohr and $b_R < 20$ Bohr.

Of course, an overwhelming majority of the nascent bound pairs of the Cs^+ and Br^- ions in our calculations possessed a rather noticeable amount of internal energy. The a priori minimal total internal energy of the ionic pair corresponds to motionless tangent balls representing the Cs^+ and Br^- ions and is equal to $E_\omega = -3.966842$ eV. In our calculations, the proportion of the recombinative three-body collisions for which the total internal energy $E_{tot} < 0$ of the resulting bound ionic pair exceeded $E_\omega/20 = -0.198342$ eV ranged between 19.15 and 53.85% depending on R, E_i, E_R, and the case under consideration (**1** or **2**).

The question at what maximal values of the impact parameters b_i and b_R recombination is possible is rather non-trivial. In test calculations performed in quasiclassical trajectory simulation of the reaction (1) with R = Xe [13], we observed recombination neither for $b_i > 40$ Bohr nor for $b_R > 20$ Bohr, and this fact was the reason why the values $b_{i\,max} = 40$ Bohr and $b_{R\,max} = 20$ Bohr were used in the paper [13]. On the other hand, in the works [12, 19], we carried out a purposeful analysis (making use of a special algorithm) of the region of the occurrence of recombination in the space of the kinematic parameters in trajectory calculations. It was found that even for central approaches of the ions ($b_i \equiv 0$), recombination (1) for R = Xe and Hg at low energies E_i and E_R is possible at very large values of the impact parameter b_R of the third body, up to 40.5 Bohr (but to such values of b_R, there correspond very narrow intervals of the Θ and Φ angles).

It has not been our goal in the present paper to determine the extreme values of the parameters b_i and b_R for which recombination can occur within the hard sphere model. The similarity of the dependences of the recombination probability P on the energies E_i and E_R in cases **1** and **2** (for each of the four atoms R) mentioned above indicates that, in principle, one could have confined oneself with considering case **1** to figure out characteristic features of the "hard sphere" recombination dynamics. Nevertheless, impact parameters b_i between 40 and 80 Bohr and impact parameters b_R between 20 and 40 Bohr also contribute to the reactions (3). Indeed, otherwise the probability ratio $\lambda = P(\text{case } \mathbf{1})/P(\text{case } \mathbf{2})$ for all R, E_i, and E_R would be approximately equal to $2^2 \times 2^2 = 16$. Actually this ratio, with few exceptions (however, the lighter the atom R is, the larger is the number of these exceptions), lies between 7.3 and 9.3. The minimal value of the ratio λ we met with is equal to 6.484, while the maximal one is equal to 18.417 (large values of this ratio are typical for low energies E_R). At $E_i = E_R = 1$ eV, the ratio λ is equal to 7.572, 7.183, 6.957, and 7.006 for R = Hg, Xe, Kr, and Ar, respectively (see Table 1). The mean value of the ratio λ over all the 100 energy pairs (E_i, E_R) is equal to 8.383, 8.266, 8.369, and 8.933 for R = Hg, Xe, Kr, and Ar, respectively.

That three-body collisions with impact parameters b_i between 40 and 80 Bohr or with impact parameters b_R between 20 and 40 Bohr make a rather noticeable contribution to recombination can also be deduced from a straightforward analysis of the opacity functions. Consider the values

$$p_i^* = P^{part}(b_{i\,max} - 1 \text{ Bohr})$$

and

$$p_R^* = P^{part}(b_{R\,max} - 1 \text{ Bohr})$$

of the opacity functions at the middle of the last subinterval for the impact parameter b_i of ion approach and for the impact parameter b_R of the third body, respectively. In Table 1 for R = Hg, Xe, Kr, Ar and for both cases **1** and **2**, we present the quantities p_i^* and p_R^* at $E_i = E_R = 1$ eV as well as the mean values of these quantities over all the energy pairs (E_i, E_R). As is seen in Table 1, although the numbers p_i^* and p_R^* in case **2** are systematically much smaller than those in case **1**, they are nevertheless not negligibly small. The opacity functions for both the impact parameters b_i and b_R within the hard sphere model are characterized by much longer "tails" than in trajectory calculations.

One more way to estimate the "tails" of the opacity functions consists in considering the ratios

$$q_i^* = 100\frac{N_0^{part}(b_{i\,max} - 1 \text{ Bohr})}{N_0}$$

and

$$q_{\mathrm{R}}^{*} = 100\frac{N_0^{part}(b_{\mathrm{R}max} - 1\ \mathrm{Bohr})}{N_0},$$

which express the proportions (in per cent) of the recombinative three-body collisions for which the impact parameter b_{i} or the impact parameter b_{R}, respectively, lie in the last subinterval. In Table 1 for R = Hg, Xe, Kr, Ar and for both cases **1** and **2**, we present the numbers q_{i}^{*} and q_{R}^{*} at $E_{\mathrm{i}} = E_{\mathrm{R}} = 1$ eV as well as the mean values of these numbers over all the energy pairs $(E_{\mathrm{i}}, E_{\mathrm{R}})$. As is seen in Table 1, the numbers q_{i}^{*} and q_{R}^{*} in case **2** are systematically smaller than those in case **1**, but they are of the same order of magnitude (this refers especially to q_{R}^{*}).

There is the trend of a shift to the right of the maximum of the opacity function $P^{part}(b_{\mathrm{i}})$ for the impact parameter b_{i} of ion approach as the atom R mass decreases. For R = Hg, for most of the pairs $(E_{\mathrm{i}}, E_{\mathrm{R}})$, the function $P^{part}(b_{\mathrm{i}})$ attains its maximum at $b_{\mathrm{i}} = 1$ or 3 Bohr in case **1** and at $b_{\mathrm{i}} = 3$ Bohr in case **2**. For R = Ar in case **1** and for R = Kr, Ar in case **2**, for many pairs $(E_{\mathrm{i}}, E_{\mathrm{R}})$, the function $P^{part}(b_{\mathrm{i}})$ attains its maximum at rather large values of b_{i} equal to 11, 13, or 15 Bohr. The opacity function $P^{part}(b_{\mathrm{R}})$ for the impact parameter b_{R} of the third body does not exhibit such a trend. Only note that the situations where the maximum of the function $P^{part}(b_{\mathrm{R}})$ is attained at the smallest value $b_{\mathrm{R}} =$ 1 Bohr of the impact parameter are much more typical for case **1** than for case **2**.

The functions $P^{part}(\Theta)$ and $P^{part}(\Phi)$ which express the dependence of the recombination probability on the Θ and Φ angles exhibit *bimodality* for some R, E_{i}, and E_{R}, i.e., the presence of two distinct maxima. To automate an analysis of a large collection of such functions (recall that in each of cases **1** and **2**, recombination was simulated for four atoms R and for 100 energy pairs $(E_{\mathrm{i}}, E_{\mathrm{R}})$), one needs formal and easily computable measures of bimodality for sequences of numbers $(x_1, x_2, \ldots, x_n)$. Several measures of this kind have been described in the literature (see e.g. the review [43]). As a rule, those measures are based on calculating the skewness and excess coefficients of the sequence at hand (these coefficients are discussed in e.g. the manual [44]). In the present paper, we have used a more visual measure of bimodality of a sequence of numbers (this measure is probably new).

Let $(x_1, x_2, \ldots, x_n)$ be a sequence of non-negative numbers $(n \geq 2)$. A term x_j of this sequence is a non-strict local maximum whenever $x_j \geq \max(x_{j-1}, x_{j+1})$; for $j = 1$ or $j = n$, the inequalities $x_1 \geq x_2$ or $x_n \geq x_{n-1}$, respectively, should be valid. If the sequence possesses just a single local maximum, then the degree β of its bimodality is regarded as being zero. Let the number of the local maxima be larger than one. Consider an arbitrary pair (x_k, x_m) of local maxima $(k < m)$. To each such pair, assign the number α_{km} in the following way. If $m = k + 1$, then $\alpha_{km} = 0$. On the other hand, if $m \geq k + 2$, then denote by $x_{km}^{min} = \min(x_k, x_m)$ the minimum of the two numbers x_k and x_m and set

$$\alpha_{km} = \frac{100C_{km}}{C_{km} + X}, \qquad (6)$$

where

$$X = \sum_{j=1}^{n} x_j > 0, \quad C_{km} = \sum_{j=k+1}^{m-1} \max(0, x_{km}^{min} - x_j).$$

In other words, each term x_j of the sequence with index j intermediate between k and m makes a contribution to C_{km} equal to $x_{km}^{min} - x_j$ if $x_j < x_{km}^{min}$ and equal to zero otherwise. The factor 100 in the formula (6) has been chosen for convenience reasons. The degree β of bimodality of the sequence $(x_1, x_2, \ldots, x_n)$ will be defined to be the largest of the numbers α_{km} over all the pairs (x_k, x_m) of local maxima. It is easy to see that the bimodality degree β ranges between 0 and 100 and does not change as one multiplies all the terms of the sequence by one and the same positive number. On the other hand, if one adds one and the same number $\delta > 0$ to all the terms of the sequence, the bimodality degree β will either remain to be zero or decrease because after such an action, all the values C_{km} will remain unchanged whereas X will increase by $n\delta$. One can show that β is a continuous function of the numbers $x_1, x_2, \ldots, x_n$.

If the number of well pronounced maxima of the sequence is greater than two, then the value of β for such a sequence is rather large as well, but all the bimodality measures considered in the review [43] probably possess this property. It is not hard to generalize the bimodality degree β to distributions defined on an interval rather than on a discrete set.

The probability distribution $P^{part}(b_{\mathrm{i}})$ consists of $n =$ 20 numbers in case **1** and of $n = 40$ numbers in case **2**. The probability distribution $P^{part}(b_{\mathrm{R}})$ consists of $n = 10$ numbers in case **1** and of $n = 20$ numbers in case **2**. The probability distribution $P^{part}(\Theta)$ always consists of $n =$ 36 numbers. One can estimate the bimodality degree of these distributions straightforwardly by calculating the quantity β. An analysis of the probability distribution $P^{part}(\Phi)$ which always consists of $n = 36$ numbers as well is more delicate. The reason is that the periodicity of the spherical frame in the azimuthal angle Φ can give an illusion of bimodality which is absent in reality. For example, suppose that the probabilities

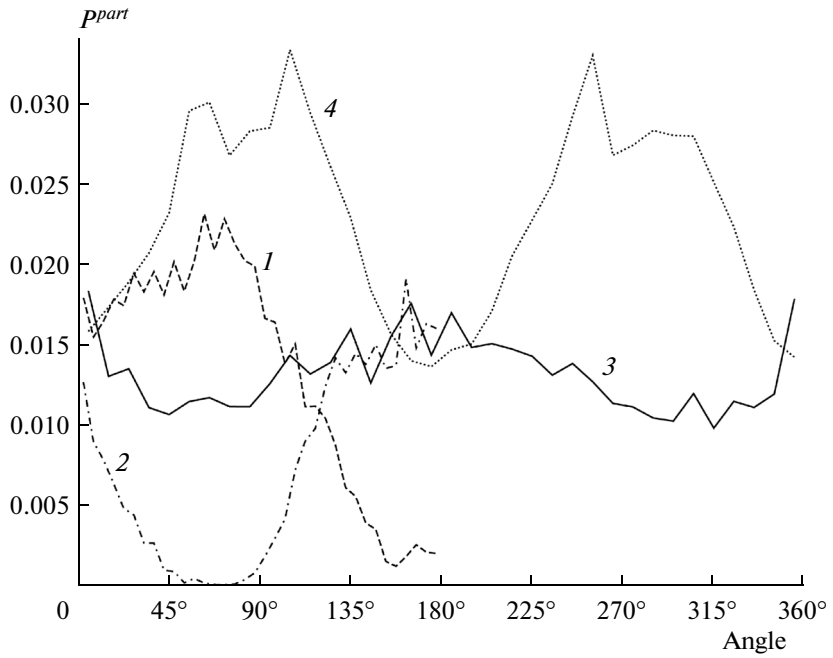

Fig. 3. Some dependences of the recombination probability on the Θ and Φ angles in case **1**. Line *1* is the unimodal function $P^{part}(\Theta)$ for R = Hg at $E_i = E_R = 4$ eV with $\beta = 0.93$. Line *2* is the sharply bimodal function $P^{part}(\Theta)$ for R = Ar at $E_i = E_R = 6$ eV with $\beta = 44.74$. Line *3* is the weakly bimodal function $P^{part}(\Phi)$ for R = Xe at $E_i = 6$ eV and $E_R = 3$ eV with $\beta = 26.21$ and $\tilde{\beta} = 13.17$. Line *4* is the bimodal function $P^{part}(\Phi)$ for R = Kr at $E_i = 2$ eV and $E_R = 6$ eV with $\beta = \tilde{\beta} = 17.76$.

$P^{part}(\Phi)$ are large for angles Φ close to 0° and to 360° and are small for the intermediate angles. Such a probability distribution seems to be bimodal but in fact it has the only maximum at the point Φ = 0°. Indeed, if the values of the kinematic parameters E_i, E_R, b_i, b_R, Θ, γ are fixed then, as Φ → 0° and as Φ → 360°, we are approaching, from different directions, the same collection of initial conditions of a three-body collision of the particles (see Section 2). A similar phenomenon is also possible for a larger number of maxima. For instance, if the distribution of recombination probabilities with respect to Φ admits two maxima at the points Φ = 0° and Φ = 180°, then the impression can be created that there are three maxima (such situations are exemplified by line *3* in Fig. 3). Therefore, as the bimodality degree of the distribution $P^{part}(\Phi)$, one has to use the minimum of the quantities β corresponding to this sequence itself and to all its 35 cyclic permutations. We will denote this bimodality measure by $\tilde{\beta}$. Recall that the cyclic permutations (or cyclic shifts) of a sequence $(x_1, x_2, \ldots, x_n)$ are by definition the $n-1$ sequences $(x_2, x_3, \ldots, x_n, x_1)$, $(x_3, x_4, \ldots, x_n, x_1, x_2)$, …, $(x_n, x_1, x_2, \ldots, x_{n-1})$ [45].

In Table 1 for R = Hg, Xe, Kr, Ar and for both cases **1** and **2**, we present the bimodality degrees β of the probability distributions $P^{part}(b_i)$, $P^{part}(b_R)$, $P^{part}(\Theta)$ and the bimodality degree $\tilde{\beta}$ of the distribution $P^{part}(\Phi)$. The bimodality degrees are averaged over all the energy pairs (E_i, E_R).

It is seen in Table 1 that the opacity functions are bimodal neither for b_i nor for b_R, on the whole. The bimodality degrees of the distributions of recombination probabilities with respect to the Θ and Φ angles are significantly higher on the average, especially in case **2**. For some R, E_i, and E_R, the quantity β for $P^{part}(\Theta)$ attains a value of 30 or even 50. The region of high values of β for $P^{part}(\Theta)$ on the (E_i, E_R) plane is approximately a wide strip parallel to the straight line $E_i = E_R$. This strip shifts towards the point $E_i = 10$ eV, $E_R = 1$ eV as the mass of the atom R increases. The quantity $\tilde{\beta}$ for $P^{part}(\Phi)$ for some R, E_i, and E_R attains a value of 35 or 40. High values of $\tilde{\beta}$ are typical mainly for low energies E_i as well as (for R = Kr and Ar) for low energies E_R.

As an example, Fig. 3 shows two functions $P^{part}(\Theta)$ and two functions $P^{part}(\Phi)$ in case **1** for various R, E_i, and E_R. The small oscillations in these dependences are due to statistical inaccuracies.

Note that in trajectory simulation of the reaction (1) with R = Xe for non-central approach of the ions, the typical distributions of recombination probability with

respect to the impact parameter b_R of the third body and to the Θ angle turn out to be unimodal (i.e., each of them has a single distinct maximum) and those with respect to the Φ angle turn out to be bimodal [13, 18]. In contrast to that, for central approach of the ions ($b_i \equiv 0$), the "trajectory" distributions of recombination probability with respect to b_R are bimodal for any of the atoms R = Hg, Xe, Kr [8–10, 13] (the two maxima in these distributions correspond to two different recombination mechanisms).

4. TYPES OF THREE-BODY COLLISIONS

In an analysis of the dynamics of direct three-body recombination by the quasiclassical trajectory method, a description of the configurations of the three particles during energy transfer from the ionic pair to the third body plays a great role [7–20]. In hard sphere simulation of recombination, three-body configurations have only kinematic meaning but not dynamical one, because the atom R interacts with each of the ions at the instant of direct contact only. On the other hand, for each three-body collision event, the hard sphere model enables one to determine absolutely unambiguously the sequence of pairwise encounters of the balls representing the particles Cs^+, Br^-, and R. Treating the Cs^+ ion as the first particle, the Br^- ion as the second one, and the atom R as the third one, we will encode any such encounter by one of the six numbers 12, −12, 13, −13, 23, and −23 according to the following rule. An encounter of the ions with each other is denoted by one of the numbers 12 or −12, an encounter of the Cs^+ ion with the atom R, by one of the numbers 13 or −13, an encounter of the Br^- ion with the atom R, by one of the numbers 23 or −23, while the sign of the number coincides with the sign of the total internal energy E_{tot} of the ionic pair after the encounter.

Any recombinative three-body collision includes at least one encounter of the code −13 or −23, and after all the encounters of the atom R with the ions, some more encounters of the ions with each other of the code −12 are possible. Within the framework of a non-recombinative three-body collision, after all the encounters of the atom R with the ions, one more encounter of the ions with each other of the code 12 is possible. While assigning a sequence of the numbers encoding the pairwise encounters of the particles to a three-body collision, we will not take into account these final encounters of the ions with each other (they do not change the total internal energy of the ionic pair). The sequence of numbers thus obtained will be called the *type* of the three-body collision.

For instance, a collision of the type (13, −23) is recombinative and includes an encounter of the Cs^+ ion with the atom R leaving the energy E_{tot} positive, an encounter of the Br^- ion with the atom R changing the sign of the energy E_{tot}, and possibly some more encounters of the ions with each other of the code −12. A non-recombinative collision of the type ∅ (an empty sequence) either does not include encounters of the particles at all or includes the only encounter of the code 12. The "longest" type we met with was the sequence (23, 23, 23, 23, 23, 23, 23, 23, 23). We observed only one collision of this type, and during that non-recombinative collision, nine encounters of the Br^- ion with the Hg atom occurred.

Table 3. The fifteen most frequently occurring types of non-recombinative three-body collisions

Number of collisions	In per cent	Type
337533617	85.04	∅
29165971	7.348	(13)
27248230	6.865	(23)
1166056	0.294	(23, 13)
925488	0.233	(13, 23)
439401	0.111	(12, 23)
223502	0.0563	(12, 13)
59961	0.0151	(−23, 13)
39858	0.0100	(−13, 23)
32631	0.0082	(13, 12, 23)
23868	0.0060	(23, 13, 23)
21507	0.0054	(23, 12, 23)
14709	0.0037	(23, 12, 13)
14603	0.0037	(13, 23, 13)
11634	0.0029	(13, 12, 13)

The number of collisions in per cent is given with respect to the total number of non-recombinative collisions, 396929511.

Of course, as a result of a recombinative three-body collision, a bound ionic pair remains after all the encounters of the atom R with the ions, and in this pair, either no encounters of the ions with each other occur at all or the ions undergo infinitely many encounters. However, before the termination of integrating the equations of motion according to the algorithm presented in Section 2, only a finite number (usually no greater than ten) of such encounters of the code −12 have time to happen. The maximal number of such encounters in our calculations took place for one of the collisions with R = Kr and was equal to 1324.

All the totality of the calculations described in this work comprises $N_{all} = 2 \times 4 \times 100 \times 500000 = 4 \times 10^8$ three-body collision events, here one takes into account two cases (**1** and **2**), four different atoms R, and 100 energy pairs (E_i, E_R). Of these 4×10^8 three-body collisions, 3070489 collisions (0.7676%) of 34 different types turned out to be recombinative. All the types of recombinative collisions we observed are listed in Table 2 (in the descending order of the numbers of collisions belonging to the types in question). In this table as well as in Table 3 below, we present exact numbers of collisions of various types we met with in

our calculations. If the proportion of the collisions of a certain type among all the N_{all} collisions turns out to be equal to η $(0 < \eta < 1)$, then the statistical inaccuracy of the quantity η is of the order $[\eta(1-\eta)/N_{all}]^{1/2}$ [44].

As is seen in Table 2, an overwhelming majority (84.0893%) of recombinative collisions belong to the types (−23) and (−13). Collisions of these types include the only encounter of the atom R with one of the ions (without a preceding encounter of the ions with each other possible for small values of b_i only). As a result of this encounter, excess energy transfers from the ionic pair to the neutral atom. The energy removal occurs more frequently in an encounter of the atom R with the Br^- ion than in that with the Cs^+ ion, which is due to two reasons. First, a Br^- ion is lighter than a Cs^+ ion, so that in an encounter with the third body, the velocity of the Br^- ion changes stronger on the average (and, consequently, the relative velocity of the two ions and the total internal energy E_{tot} of the ionic pair change stronger as well). Second, the ionic radius of a Br^- ion is larger than that of a Cs^+ ion [30], so that it is easier for the atom R to "touch" the Br^- ion. The next in frequency are the collision types (13, −23) and (23, −13) corresponding to the situation where the atom R encounters first one of the ions and then the other ion, and excess energy transfers from the ionic pair to the neutral atom at the instant of the second encounter. The four types just mentioned put together cover 93.7319% of all the recombinative collisions.

The number of different types of non-recombinative three-body collisions we observed was equal to 61. The fifteen most frequently occurring types are listed in Table 3 (in the descending order of the numbers of collisions belonging to the types in question). These 15 types cover 99.9979% of all the non-recombinative collisions. An overwhelming majority (85.0362%) of non-recombinative collisions belong to the type $\varnothing$ (the neutral atom R flies past the ionic pair without having "touched" any of the ions). The dynamics of non-recombinative collisions of the types (−23, 13) and (−13, 23) is of special interest. Such collisions correspond to the situation where an impact of the atom R with one of the ions stabilizes the ionic pair, but after the subsequent encounter of the atom R with the other ion the total internal energy E_{tot} of the ionic pair becomes positive again.

Table 1 presents the proportions of the three-body collisions of the types (−13) and (−23) among all the recombinative collisions with a given atom R within the framework of one of cases **1** and **2**. These proportions are denoted by Z_{-13} and Z_{-23}. As is seen in Table 1, the lighter the third body R is, the smaller is the proportion of the collisions of the type (−13) among all the recombinative three-body collisions and the larger is the proportion of the collisions of the type (−23). Indeed, the smaller the mass of the atom R is, the more slightly on the average the total internal energy E_{tot} of the ionic pair changes at an encounter of this atom with one of the ions. Such an effect takes place for both the ions, but it is pronounced much stronger at encounters of R with the heavy ion Cs^+ than at encounters of R with the lighter ion Br^-. Therefore, as the mass of the atom R decreases, the role of the encounters of R with Br^- in the recombination process increases and the role of the encounters of R with Cs^+ falls off, although the inequality $Z_{-13} < Z_{-23}$ holds even for the heaviest third body R = Hg.

The relative contributions of the three-body collisions of the types (−13) and (−23) to the total recombination probability depend very strongly on the ion approach energy E_i and the third body energy E_R. A possible reason is that for some energy pairs (E_i, E_R), the encounter of the atom R with the ion occurs mainly when the ions approach each other, whereas for the other pairs, it happens when the ions move away from each other. Denote by $\zeta_{-13}(E_i, E_R)$ and $\zeta_{-23}(E_i, E_R)$ the proportions of the three-body collisions of the types (−13) and (−23), respectively, among all the recombinative collisions (3) with a given atom R and given energies E_i and E_R within the framework of one of cases **1** and **2**. As the energy E_i increases, the quantity $\zeta_{-13}(E_i, E_R)$ decreases on the whole while the quantity $\zeta_{-23}(E_i, E_R)$ grows. As the energy E_R increases, the opposite trends are observed, namely, the quantity $\zeta_{-13}(E_i, E_R)$ grows on the whole while the quantity $\zeta_{-23}(E_i, E_R)$ falls off. It is not hard to express these trends in a quantitative form. The inequality $\zeta_{-13}(E_i + 1\text{ eV}, E_R) < \zeta_{-13}(E_i, E_R)$ holds in 590 situations out of $2 \times 4 \times 10 \times 9 = 720$, here one takes into account two cases (**1** and **2**), four different atoms R, 10 values of the energy E_R, and 9 values of the energy E_i. The inequality $\zeta_{-23}(E_i + 1\text{ eV}, E_R) > \zeta_{-23}(E_i, E_R)$ holds in 611 situations out of 720. The inequality $\zeta_{-13}(E_i, E_R + 1\text{ eV}) > \zeta_{-13}(E_i, E_R)$ holds in 624 situations out of 720, and the inequality $\zeta_{-23}(E_i, E_R + 1\text{ eV}) < \zeta_{-23}(E_i, E_R)$ holds in 592 situations out of 720.

For high values of E_R and low values of E_i, the proportion $\zeta_{-13}(E_i, E_R)$ usually exceeds $\zeta_{-23}(E_i, E_R)$, especially for R = Hg, Xe, and Kr, despite the inequality $Z_{-13} < Z_{-23}$ which expresses the relation between the contributions of the collisions of the types (−13) and (−23) after summing over the energies. On the contrary, for high values of E_i and low values of E_R, very small (less than 10%) values of the quantity $\zeta_{-13}(E_i, E_R)$ are typical. The lighter the third body R is, the more pronounced is this effect. For instance, for R = Ar in case **1** for the energy pairs (E_i, E_R) = (4, 1), (5, 1), (6, 1), (6, 2), (7, 1), (7, 2), (7, 3), (8, 1), (8, 2), (8, 3), (9, 1), (9, 2), (9, 3), (9, 4), (10, 1), (10, 2), (10, 3), (10, 4), and (10, 5) (in eV), we observed no recombinative collisions of the type (−13) at all.

5. CONCLUSIONS

The calculations we carried out have shown that the hard sphere model allows one to reproduce many characteristic features of the dynamics of direct three-body recombination of ions, in particular, the shape of the dependence $P(E_i, E_R)$ of the total recombination probability P on the ion approach energy E_i and the third body energy E_R, unimodal opacity functions in the impact parameter b_R of the third body, and bimodal dependences of the recombination probability on the azimuthal angle Φ. This implies that one can certainly use the hard sphere model to clarify those aspects of the three-body recombination dynamics that are difficult to be separated "in pure form" in quasiclassical trajectory calculations. Although, as a research tool, hard sphere simulation is much cruder than the conventional method of classical trajectories, the essential advantages of hard sphere models are, first, a higher speed of calculations, second, the possibility of studying mass and orientation effects irrespective of the PES topography, third, the possibility of an unambiguous classification of the collisions according to the sequences of pairwise encounters of the particles (an analogous classification of the trajectories cannot be performed without a certain arbitrariness), and fourth, visuality [27].

In the present paper, we have not employed these advantages to a full extent, because we examined the recombination reaction mainly on the statistical level, with a selection of the kinematic parameters of the collision according to the formulas (5). In recent years, within the framework of the classical trajectory method, the detailed dynamics of elementary processes (dynamics within a single trajectory) has been developed, where averaging over kinematic parameters is reduced to a minimum or absent at all [8, 11, 14, 15, 18–20, 46]. What can be the hard sphere analogue of the detailed dynamics of a reaction is the *detailed kinematics*, i.e., an analysis of the evolution of the mutual arrangement of the particles (in our situation, the particles are the ionic pair and the third body which moves under no forces in the time intervals between the encounters with the ions) during a single collision event. We are going to carry out such an analysis in subsequent publications. In particular, it will hopefully enable one to explain the dependences of the relative contributions of recombinative collisions of various types on the energies E_i and E_R.

The authors are grateful to V. M. Azriel for fruitful discussions.

The work was financially supported by the Russian Foundation for Basic Research (project no. 14-03-00201-a) and by the Council for Grants of the President of the Russian Federation for state support of the leading scientific schools of the Russian Federation (grant no. NSh-5138.2014.1).

REFERENCES

1. D. L. Baulch, C. J. Cobos, R. A. Cox, et al., J. Phys. Chem. Ref. Data **21**, 411 (1992).
2. R. T. Pack, R. B. Walker, and B. K. Kendrick, J. Chem. Phys. **109**, 6701 (1998).
3. G. A. Parker, R. B. Walker, B. K. Kendrick, and R. T. Pack, J. Chem. Phys. **117**, 6083 (2002).
4. R. T. Pack, R. B. Walker, and B. K. Kendrick, J. Chem. Phys. **109**, 6714 (1998).
5. R. T. Pack, R. B. Walker, and B. K. Kendrick, J. Chem. Phys. **113**, 1668 (2000).
6. F. D. Colavecchia, F. Mrugala, G. A. Parker, and R. T. Pack, J. Chem. Phys. **118**, 10387 (2003).
7. V. M. Azriel and L. Yu. Rusin, Fiz. Khim. Kinet. Gaz. Dinam. **6** (2006). http://chemphys.edu.ru/article/36/
8. V. M. Azriel, D. B. Kabanov, L. I. Kolesnikova, and L. Yu. Rusin, Izv. Akad. Nauk, Energet., No. 5, 50 (2007).
9. V. M. Azriel and L. Yu. Rusin, Russ. J. Phys. Chem. B **2**, 499 (2008).
10. V. M. Azriel, Doctoral Dissertation in Mathematics and Physics (Inst. Energy Problems Chemical Physics of RAS, Moscow, 2008).
11. D. B. Kabanov and L. Yu. Rusin, Fiz. Khim. Kinet. Gaz. Dinam. **8** (2009). http://chemphys.edu.ru/article/142/
12. E. V. Kolesnikova, D. B. Kabanov, and L. Yu. Rusin, Fiz. Khim. Kinet. Gaz. Dinam. **10** (2010). http://chemphys.edu.ru/article/153/
13. V. M. Azriel, E. V. Kolesnikova, L. Yu. Rusin, and M. B. Sevryuk, J. Phys. Chem. A **115**, 7055 (2011).
14. D. B. Kabanov and L. Yu. Rusin, Chem. Phys. **392**, 149 (2012).
15. D. B. Kabanov and L. Yu. Rusin, Russ. J. Phys. Chem. B **6**, 475 (2012).
16. E. V. Kolesnikova and L. Yu. Rusin, Fiz. Khim. Kinet. Gaz. Dinam. **13** (2012). http://chemphys.edu.ru/article/274/
17. E. V. Kolesnikova and L. Yu. Rusin, Russ. J. Phys. Chem. B **6**, 583 (2012).
18. V. M. Azriel, L. Yu. Rusin, and M. B. Sevryuk, Chem. Phys. **411**, 26 (2013).
19. E. V. Ermolova, Candidate's Dissertation in Mathematics and Physics (Inst. Energy Problems Chemical Physics of RAS named by V. L. Tal'roze, Moscow, 2013).
20. E. V. Ermolova and L. Yu. Rusin, Russ. J. Phys. Chem. B **8**, 261 (2014).
21. B. H. Mahan, W. E. W. Ruska, and J. S. Winn, J. Chem. Phys. **65**, 3888 (1976).
22. S. A. Safron, J. Phys. Chem. **89**, 5713 (1985).
23. A. I. Maergoiz, E. E. Nikitin, and L. Yu. Rusin, in *Chemistry of Plasma*, No. 12, Ed. by B. M. Smirnov (Energoatomizdat, Moscow, 1985), p. 3 [in Russian].
24. J.-B. Song, E. A. Gislason, and M. Sizun, J. Chem. Phys. **102**, 4885 (1995).
25. V. M. Azriel, L. Yu. Rusin, and M. B. Sevryuk, Khim. Fiz. **14** (7), 28 (1995).
26. V. M. Azriel, L. Yu. Rusin, and M. B. Sevryuk, Chem. Phys. **199**, 195 (1995).

27. M. B. Sevryuk, Doctoral Dissertation in Mathematics and Physics (Inst. Energy Problems Chemical Physics of RAS, Moscow, 2003).
28. V. M. Azriel, L. Yu. Rusin, and M. B. Sevryuk, J. Chem. Phys. **122**, 074322 (2005).
29. J. Pérez-Ríos, S. Ragole, J. Wang, and C. H. Greene, J. Chem. Phys. **140**, 044307 (2014).
30. P. Brumer, Phys. Rev. A **10**, 1 (1974).
31. *Chemical Encyclopedy* (Bol'sh. Rossiisk. Entsiklopediya, Moscow, 1995), Vol. 4 [in Russian].
32. *Chemical Encyclopedy* (Sovetsk. Entsiklopediya, Moscow, 1990), Vol. 2 [in Russian].
33. *Chemical Encyclopedy* (Sovetsk. Entsiklopediya, Moscow, 1988), Vol. 1 [in Russian].
34. L. D. Landau and E. M. Lifshitz, *Course of Theoretical Physics*, Vol. 1: *Mechanics* (Fizmatlit, Moscow, 2004, 5th ed.; Pergamon Press, New York, 1988).
35. V. I. Arnold, V. V. Kozlov, and A. I. Neishtadt, *Mathematical Aspects of Classical and Celestial Mechanics* (URSS, Moscow, 2002, 2nd ed.; Springer, Berlin, 2006).
36. H. Pollard, *Mathematical Introduction to Celestial Mechanics* (Prentice-Hall, Englewood Cliffs, NJ, 1966; Inst. Komp. Issled., Izhevsk, Moscow, 2012).
37. M. Avendano, V. Martín-Molina, and J. Ortigas-Galindo, Celest. Mech. Dynam. Astron. **119**, 27 (2014).
38. A. F. Aleksandrov, L. S. Bogdankevich, and A. A. Rukhadze, *Principles of Plasma Electrodynamics*, 2nd ed. (Vyssh. Shkola, Moscow, 1988) [in Russian].
39. V. E. Golant, A. P. Zhilinskii, and I. E. Sakharov, *Principles of Plasma Physics*, 2nd ed. (Lan', St.-Petersburg, 2011) [in Russian].
40. T. G. Kolda, R. M. Lewis, and V. Torczon, SIAM Rev. **45**, 385 (2003).
41. A. S. Rykov, *System Analysis: Models and Methods of Decision Making and Search Optimization* (MISiS, Moscow, 2009) [in Russian].
42. E. V. Kolesnikova, L. I. Kolesnikova, and L. Yu. Rusin, Fiz. Khim. Kinet. Gaz. Dinam. **10** (2010). http://chemphys.edu.ru/article/215/
43. T. R. Knapp, J. Mod. Appl. Stat. Methods **6**, 8 (2007).
44. H. Cramér, *Mathematical Methods of Statistics*, 2nd ed. (Princeton Univ. Press, Princeton, NJ, 1999).
45. L. A. Kaluzhnin and V. I. Sushchanskii, *Transformations and Permutations*, 2nd ed. (Nauka, Moscow, 1985) [in Russian].
46. V. M. Azriel, D. B. Kabanov, and L. Yu. Rusin, Russ. J. Phys. Chem. B **5**, 177 (2011).